EXPERIMENTAL STUDY OF THE EFFECT OF EXTERNAL PRESSURE ON PARTICLE BED EFFECTIVE THERMAL PROPERTIES

BLANKET ENGINEERING

KEYWORDS: *solid breeder, particle beds, thermomechanics*

FATOLLAH TEHRANIAN and MOHAMED A. ABDOU
University of California, Los Angeles
Mechanical, Aerospace, and Nuclear Engineering Department
405 Hilgard Ave., Los Angeles, California 90024

Received December 3, 1993
Accepted for Publication October 21, 1994

Accurate prediction of the thermomechanical responses of particle beds in fusion blankets depends strongly on the availability of experimental data on their thermal properties as a function of the blanket operating conditions. In this study, a series of experiments is conducted to measure the effective thermal conductivity and interface conductance of single-size aluminum, beryllium, and lithium zirconate particle beds as a function of applied external load in the 0- to 1.6-MPa range. Experiments are carried out with both helium and air as cover gas over a pressure range of 30 to 760 Torr. In both the aluminum and beryllium beds, as the applied load is increased to 1.5 MPa, the effective thermal conductivity increases by a factor of ~3 to 7 in an air cover gas and by a factor of ~2 to 3 in helium. With 1.2-mm lithium zirconate particles and air or helium as the cover gas, changes in the bed thermal conductivity when the applied load is varied in the 0 to 1.6-MPa range are small and within the experimental error. The increase in the interface conductance values with applied external load shows variations similar to those of the thermal conductivity.

Based on the Hertz elastic equation and finite element models, the particle-to-particle contact areas as a function of the applied external load are evaluated and used in a predictive model by Bauer, Schlunder, and Zehner to calculate the effective thermal conductivity of a beryllium particle bed as a function of external pressure. The experimental results are in good agreement with the model predictions.

I. INTRODUCTION

Particle beds have been proposed for solid breeder ceramics and multiplier materials in fusion reactor blankets.[1-4] Knowledge of the effective bed thermal conductivity and bed-clad interface thermal conductance coefficient is essential in the design and analysis of such systems. In addition to temperature, bed conductivity and wall conductance depend on the cover gas composition and pressure and the internal stress state of the bed. These dependencies can be utilized to provide more robust thermal performance or even to actively control temperature profiles during operations.[5,6]

Over the last several decades, different groups[7-9] have devoted much effort to modeling the thermal conductivity and interface conductance coefficient of packed particle beds with good success. Experimental work for benchmarking the existing models to fusion-related data has also been going on for the past several years at the University of California, Los Angeles,[10] Kernforschungzentrum Karlsruhe,[11] Canadian Fusion Fuels Technology Project[12] (CFFTP), and Japan Atomic Energy Research Institute.[13] The available models are, in general, capable of predicting thermal properties of single-size and binary-packed beds as a function of the controlling parameters such as the solid-to-gas conductivity ratio, cover gas and cover gas pressure, surface roughness, and the particle-to-particle contact area. The value of the particle-to-particle contact area has usually been assumed to be either zero (point contact assumption) or used as a parameter for benchmarking the models with the available experimental data. The actual value of the particle-to-particle contact area, however, is a function of the contact pressures between particles, which in turn depend on the magnitude of the mechanical loads to which the particle bed is subjected. The mechanical loads could result, e.g., from the thermal expansion mismatch between the bed and the clad or irradiation swelling of the bed. Depending on the stiffness of the clad, high-pressure coolants could also apply a significant load on the particle bed.

In this study, a series of experiments was performed in which the bed effective thermal conductivity as a

function of the applied external pressure was measured. Measurements were performed for aluminum, beryllium, and lithium zirconate single-size particle beds. The choices of beryllium and lithium zirconate particle beds were based on their possible use as multiplier and breeder materials in fusion blankets. An aluminum particle bed was chosen to study the high-temperature effects while avoiding the problems associated with beryllium toxicity. For some cases, based on the measured values of the effective bed thermal conductivities, we also obtained the interface conductance coefficient between the particle bed and the stainless steel surface, as a function of the applied external loads.

A comprehensive uncertainty analysis of the experimental results was performed, and the results, in terms of mean and standard deviation values (error bars) for the effective thermal conductivities of the particle beds, are presented.

The Hertz contact equation as well as a finite element model of the beryllium particles were used to calculate the particle-to-particle contact areas. Based on the calculated particle-to-particle contact areas as a function of the applied external load, we used the Bauer, Schlunder, and Zehner[8] particle bed effective thermal conductivity model to calculate the effective thermal conductivity of a beryllium particle bed as a function of the applied load. The experimental results were then compared with the model predictions.

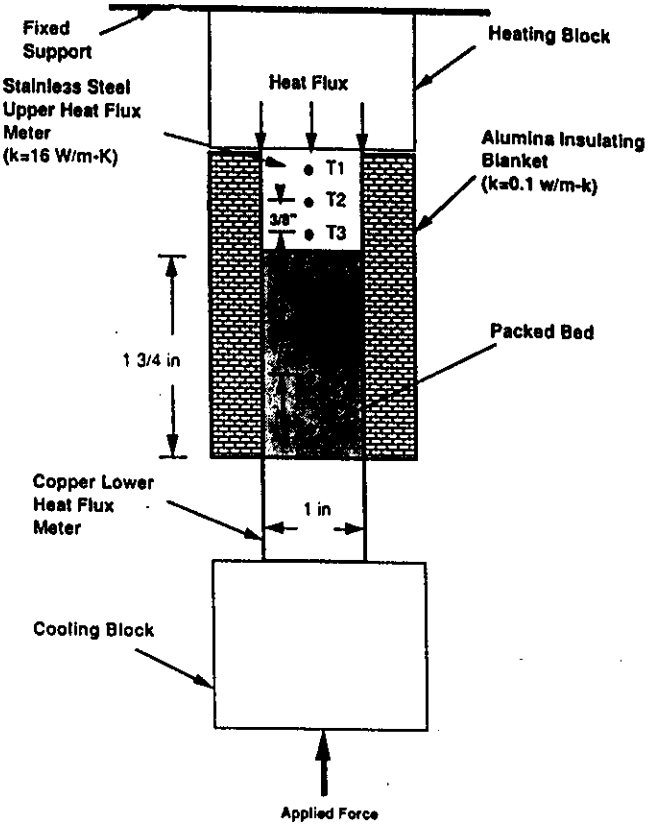

Fig. 1. Test article general configuration.

II. EXPERIMENTAL

II.A. Experimental Setup

The experimental apparatus allows control of the cover gas composition and pressure, the heat flux, and the vertical force applied to the bed. Control of the background gas is obtained by using a vacuum bell jar pumped with a mechanical force pump and backfilled with air, N_2, or helium. Up to 500 W of heat is applied by using a cable heater attached to a copper heating block. The heat then passes through a 2.54-cm rod for measuring the heat flux, through the specimen region, through another heat flux rod, and then into the water coolant. Forces are applied with a 12-t hydraulic press and measured with a standard load cell. Instrumentation includes thermocouples along the heat flux rod and in the bed, gas pressure gauges, and the load cell.

II.B. Test Article Configuration

Figure 1 shows a sketch of the test article. The test article consists of a cylindrical column of single-size particles contained in a thermal insulator sleeve made of cylindrical alumina tubes, Type AL-30.[a] The container is 5 cm long and has an inside diameter of 2.54 cm and a wall thickness of 1.27 cm. It has a thermal conductivity of ~0.09 W/m·K at 500°C and a compressive strength of ~3.4 MPa normal to the thickness. The low conductivity insulating container is used to minimize the lateral heat losses and, therefore, the uncertainty in the measured heat fluxes. The heat flux through the test article is measured by a 2.54-cm-diam stainless steel heat flux meter located on the top of the bed. The temperatures through the bed are measured at four locations. The full description of the test article and its integration with the experimental setup is given in Ref. 14

II.C. Particle Bed Materials

Figure 2 shows the scanning electron micrographs of the particles used in these experiments. Aluminum and lithium zirconate[b] particles were granular with average diameters of 0.8 and 1.2 mm, respectively. The beryllium particles[c] were spherical with an average diameter of 2 mm and surface roughness of ~1 μm. The

[a]These tubes were obtained from ZirCar Product, Inc.

[b]The lithium zirconate particles were fabricated at Atomic Energy of Canada Ltd. Chalk River Laboratories (Ontario, Canada) and provided by the CFFTP.

[c]The beryllium particles were obtained from Brush Wellman.

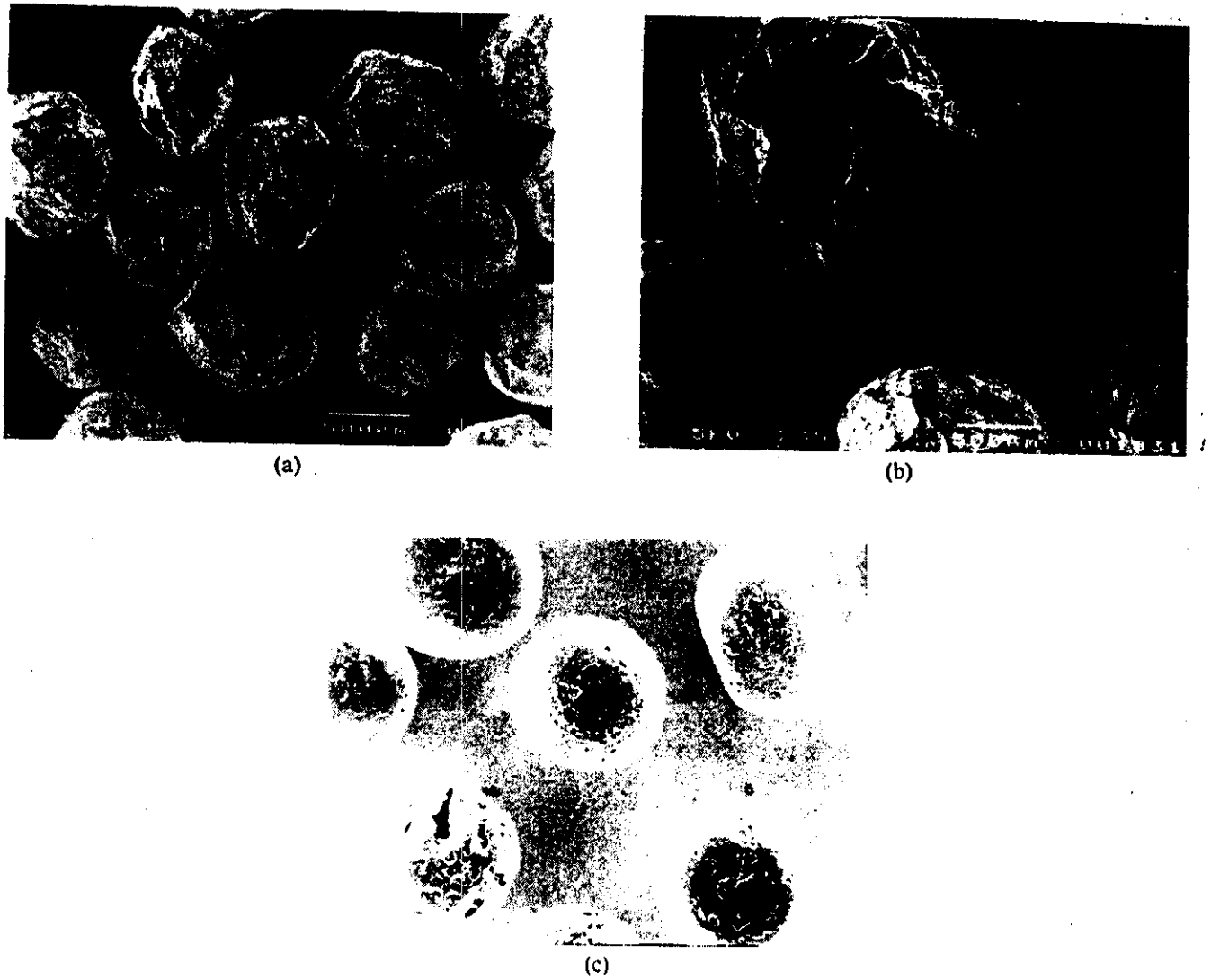

Fig. 2. Scanning electron micrographs of (a) aluminum, (b) lithium zirconate, and (c) beryllium particles.

low-purity granular aluminum particles were fabricated by chip attrition.

III. ANALYSIS

III.A. Measured Bed Effective Thermal Conductivity and Interface Thermal Conductance Coefficient

The bed effective thermal conductivity was obtained by dividing the measured heat flux through the bed q_b'', described in Sec. III.A.1, by the temperature gradient between thermocouple positions 4 and 5 (Fig. 1), namely,

$$k_{eff} = q_b'' \times \frac{Dx}{(T_4 - T_5)} , \qquad (1)$$

where Dx is the distance between the two thermocouples and T_4 and T_5 are the temperature readings of thermocouples 4 and 5.

The bed-wall interface thermal conductance coefficient h_c is defined as

$$h_c = \frac{q_i''}{(T_w - T_{bw})} , \qquad (2)$$

where

q_i'' = heat flux through the interface

T_w = steel temperature at the interface obtained by extrapolation of the measured temperature profile through the upper heat flux meter to the interface, using known steel thermal conductivity

T_{bw} = bed temperature at the interface obtained by extrapolation of the measured bed temperature profile using the measured bed thermal conductivity.

III.A.1. Measured Heat Flux at the Steel–Particle Bed Interface and through the Particle Bed

To obtain the heat flux at the upper heat flux meter–bed interface, the temperature measurements T_1, T_2, and T_3 through the upper heat flux meter (Fig. 1) are fit to a second-order equation in distance from the interface. The product of the heat flux meter thermal conductivity and the temperature gradient at the interface then gives the heat flux passing through the steel-bed interface. Equation (3) gives the heat flux at the interface in terms of the three measured temperatures and thermal conductivity k of the heat flux meter:

$$q_i'' = \left(\frac{k}{2.54 \times 10^{-2}}\right) \times \left[\frac{(2T_2 - T_1 - T_3)}{0.1607} - \frac{(4T_2 - 4T_1 - T_3)}{0.75}\right], \quad (3)$$

where q_i'' is in W/m^2 and k is in W/m·K.

Because of the lateral heat losses through the alumina container, the heat flux passing through the particle bed between thermocouple positions 4 and 5 is obtained by multiplying the heat flux at the interface given by Eq. (3) by a correction factor. The correction factor F, defined as the ratio of the heat flux through the particle bed by the heat flux at the interface, is a function of the bed thermal conductivity and the bed-wall interface thermal conductance coefficient. The values of F as a function of these two parameters were calculated by using detailed two-dimensional finite element thermal analysis of the test article[14] and are in the range of 0.88 to 1.0.

III.A.2. Uncertainty Analysis

The main contributors to the uncertainties in the bed effective thermal conductivity are the uncertainties in the heat flux through the bed q_i'', the temperature difference between thermocouple positions 4 and 5 in the bed DT, and the measured distance between the two thermocouples Dx. The uncertainties in the calculated heat flux in turn are mainly due to the uncertainties in the temperature measurements T_1, T_2, and T_3 through the upper heat flux meter. The uncertainties in the temperature measurements by the K-type thermocouples used in the experiments have been determined to be ~0.11% (Ref. 15). The uncertainty in the measured distance between thermocouple positions 4 and 5 (1.27 cm) was estimated to be <10%, or 1.27 mm. To obtain the uncertainties in the bed effective thermal conductivity values, we used the response surface method[16,17] to first calculate the uncertainties in the heat flux due to the uncertainties in the temperature measurements T_1, T_2, and T_3 through the upper heat flux meter. The calculated uncertainties in the heat flux were then used, along with the uncertainties in the thermocouple distance Dx and temperature difference DT, to obtain the uncertainties in the bed effective thermal conductivity. Calculations were repeated for all of the data points, and the results in terms of the mean values of the bed effective thermal conductivity and its variance as well as the relative contributions of the uncertainties in the heat flux, temperature difference, and distance between thermocouples are presented.

Because of the large uncertainties involved in the interface temperature drop ($T_w - T_{bw}$), which are used to calculate the interface thermal conductance coefficients as explained in Sec. III.A, the uncertainties in the interface thermal conductance coefficient values are believed to be much higher than those of the bed effective thermal conductivity.

III.B. Model Predictions for Beryllium Bed Effective Thermal Conductivity

During the last several years, extensive effort has been devoted to the modeling and prediction of particle bed effective thermal properties. The models, in general, are capable of calculating the bed effective thermal conductivity and bed-wall interface thermal conductance coefficient as a function of the parameters involved (solid-to-gas thermal conductivity ratio, cover gas, cover gas pressure, bed packing fraction, particle-to-particle contact area, etc.). The particle-to-particle contact area has usually been used as an adjustable parameter to benchmark the models against the available experimental data. In the current study, however, the particle-to-particle contact area that is a function of the contact pressure between particles is calculated by first deriving the relation between particle-to-particle contact force and the applied external load. Then, by using the calculated contact force, the contact area is calculated.

III.B.1. Particle-to-Particle Contact Area

For a cylindrical particle bed (with a cross-sectional area A, subjected to an axial external pressure P_{ext}, and assuming orthorhombic unit cell for the particles, one can write the following:

a, unit cell side = d_p

A_u, unit cell cross section = $2d_p \sin(60 \text{ deg})$

V_u, unit cell volume = $A_u \cdot a$

N, number of unit cells in $A = A/A_u$,

where d_p is the particle diameter.

For the first layer of particles in contact with the upper heat flux meter, each particle will have one point of contact with the stainless steel wall. The particle/wall contact force F_c is therefore $A * P_{ext}/N$ and is in the axial direction.

Each particle is in contact with three particles in the subsequent layer with an angle of ~35 deg between the particle-to-particle contact normal and the direction of the applied load. Therefore, the contact force between the two particles will be $(\frac{1}{3}) \times F_c \times \cos(35)$. The radius of contact for two identical particles, as a function of the contact force f_c, is give by the Hertz equation as

$$r_c = \left[\frac{3 f_c d_p (1 - u^2)}{8E}\right]^{1/3}, \quad (4)$$

where

E = modulus of elasticity

u = Poisson's ratio.

Equation (4), however, applies only in the elastic regime. To account for the effect of particle plastic deformations on the contact area, we performed detailed finite element analysis of the contact area with nonlinear material properties. The details of the particle finite element analysis is given in Ref. 15.

Table I shows the particle-to-particle contact radii for the 2-mm beryllium particles as a function of the applied external load, based on the Hertz equation as well as detailed finite element analysis. The contact radius values obtained through the finite element analysis are larger than those obtained by using the Hertz equation by a factor of ~1.3 to 1.4. The $(r_c/r_p)^2$ values based on finite element analysis, which are believed to be more accurate, along with other parameters given in Table II, were used in the bed thermal conductivity model to calculate beryllium bed effective thermal conductivity as a function of the applied external load.

TABLE I

Beryllium Particle-to-Particle Contact Radius as a Function of the Applied Load

Applied Load (MPa)	Contact Force (N)	Contact Radius (m)	
		Based on Hertz's Equation	Based on Finite Element Analysis
0.15	0.142	9.2×10^{-6}	9.6×10^{-6}
0.30	0.283	1.16×10^{-5}	12.8×10^{-6}
0.45	0.425	1.33×10^{-5}	16.03×10^{-6}
0.60	0.567	1.45×10^{-5}	19.24×10^{-6}
0.75	0.708	1.57×10^{-5}	22.45×10^{-6}
0.90	0.85	1.67×10^{-5}	24.05×10^{-6}
1.05	0.992	1.76×10^{-5}	25.65×10^{-6}
1.20	1.134	1.84×10^{-5}	27.26×10^{-6}
1.35	1.280	1.91×10^{-5}	28.86×10^{-6}
1.50	1.420	1.98×10^{-5}	28.86×10^{-6}

IV. RESULTS AND DISCUSSION

Based on the measured weight and volume of the particle beds and given particle densities of 100, 90, and 80% theoretical density, respectively, the packing fractions of the aluminum, beryllium, and lithium zirconate beds were calculated to be 63, 63, and 69%, respectively.

IV.A. Aluminum Bed Effective Thermal Conductivity

Figure 3 shows the variation in the bed effective thermal conductivity as a function of applied external load and with air and helium as the cover gas. The effective thermal conductivity of the aluminum particle bed, with air at atmospheric pressure as the cover gas, increased by a factor of 5.2 as the applied load was increased from zero to ~1.36 MPa. For the same range of the applied load (0 to 1.36 MPa), with air at 38 Torr pressure, the bed effective thermal conductivity increased by a factor of ~7.7. With helium at 1 atm and 200 Torr pressure, an increase in the applied load from zero to 1 MPa increased the bed effective thermal conductivity by a factor of 1.86 and 2.4, respectively. It is clear that the increase in the bed effective thermal conductivity, due to the applied external load, is a strong function of the solid-to-gas conductivity ratio. The higher this ratio, the larger is the effect of the applied external load in increasing the bed effective thermal conductivity.

IV.B. Beryllium Bed Effective Thermal Conductivity

The results of the measurements on the beryllium bed effective thermal conductivity as a function of applied load, shown in Fig. 4, are similar to those of the aluminum particle bed. The bed effective thermal conductivity, with air at atmospheric pressure as the cover gas, increased by a factor of 4.64 as the applied pressure was increased from zero to ~1.22 MPa. For the same range of the applied load (zero to 1.22 MPa) and air at 34 Torr, the bed effective thermal conductivity increased from 0.23 to ~1.7 W/m·K, i.e., by a factor

TABLE II

Parameters Used in the Models

Solid beryllium conductivity (W/m·K)	150
Helium/beryllium accommodation coefficient	0.4
Helium thermal conductivity (W/m·K)	0.15
Air/beryllium accommodation coefficient	0.85
Air thermal conductivity (W/m·K)	0.028

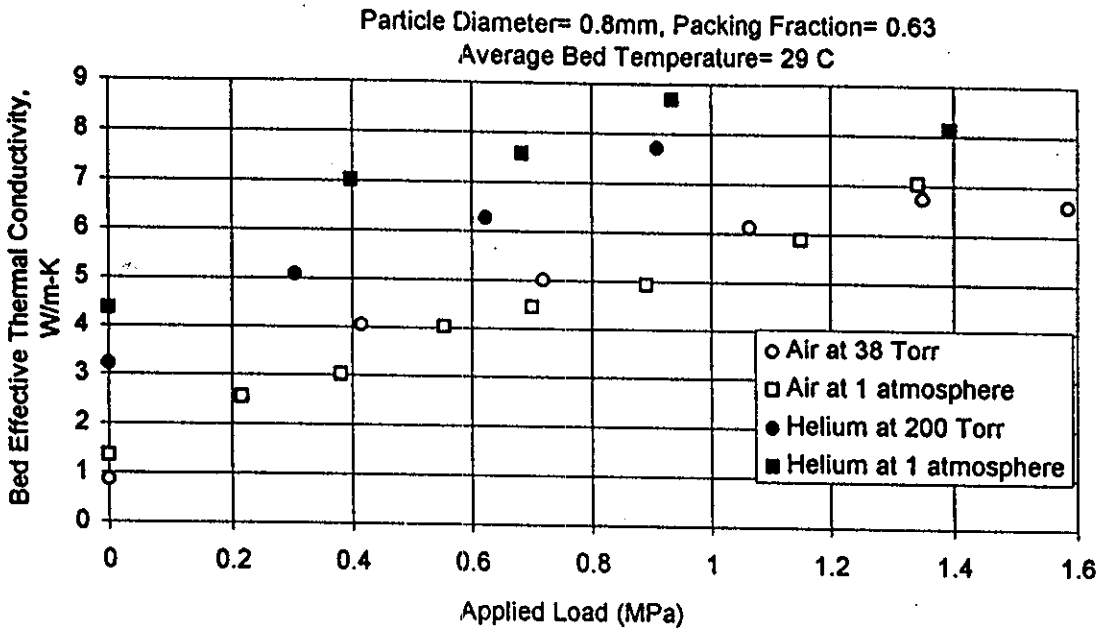

Fig. 3. Effect of external load on aluminum particle bed effective thermal conductivity.

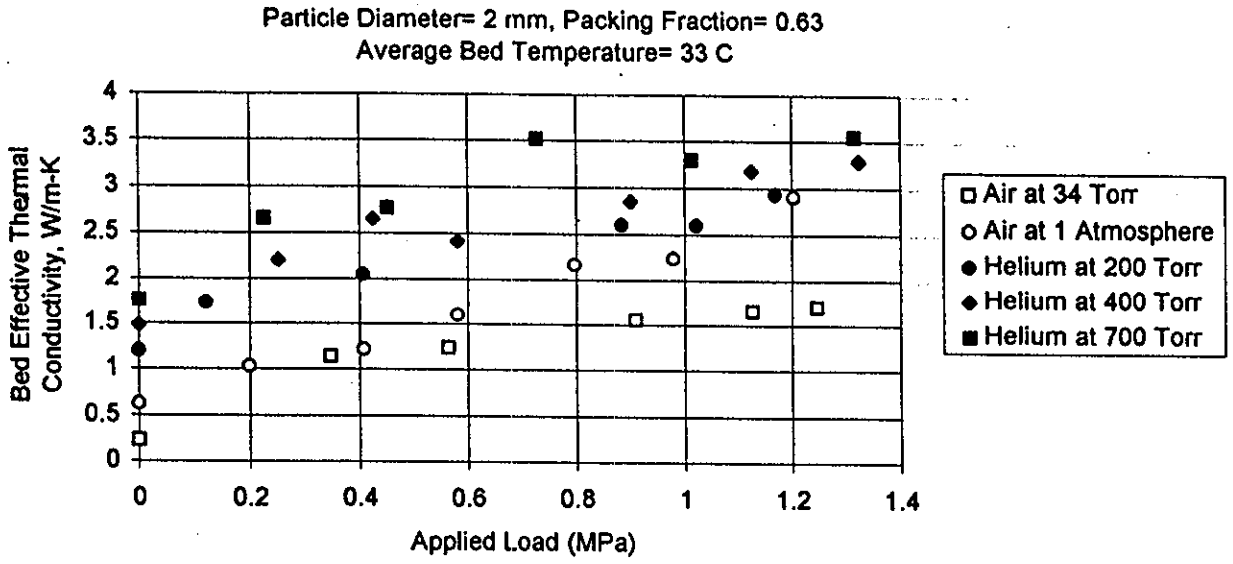

Fig. 4. Effect of external load on beryllium particle bed effective thermal conductivity.

of 7.4. With helium at 700, 400, and 200 Torr, increasing the applied load from zero to 1.22 MPa increased the bed effective thermal conductivity by a factor of ~2, 2.2, and 2.46, respectively.

IV.C. Lithium Zirconate Bed Effective Thermal Conductivity

Figures 5 and 6 show the measured lithium zirconate particle bed effective thermal conductivity as a function of the applied load in the 0- to 1.7-MPa range with air at 1 atm and 42 Torr and helium at 200, 400, and 700 Torr pressures as the cover gas. The variations in the bed effective thermal conductivity with applied load appear to be small and within the experimental error.

Table III shows the effect of external load on bed effective thermal conductivity for an arbitrary reference load value of 0.68 MPa. In Table III, the thermal conductivity ratio, defined as the bed thermal conductivity when subjected to an external load divided by the bed

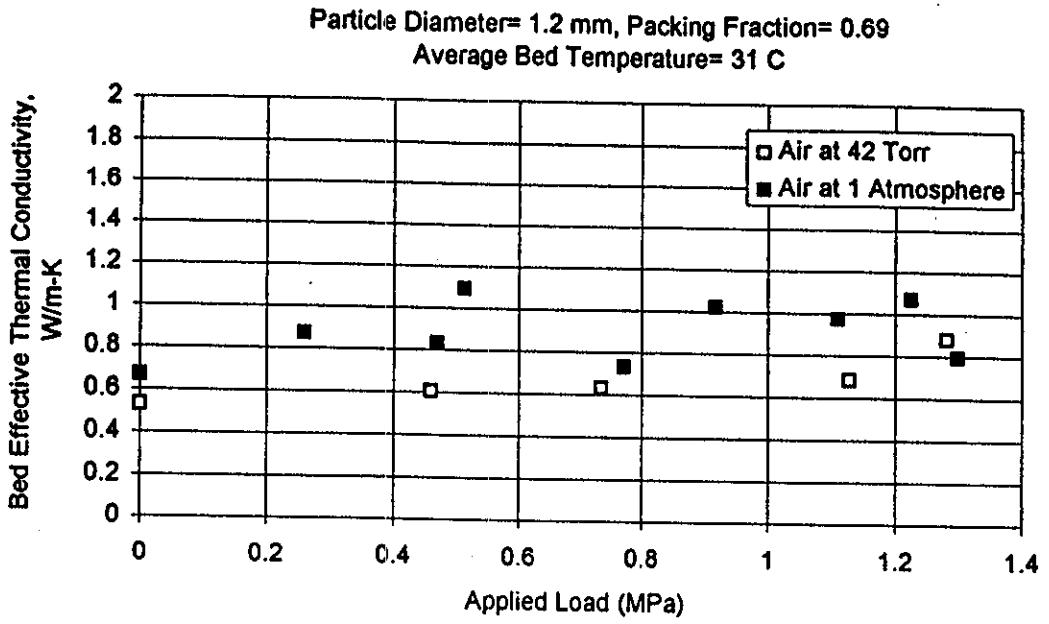

Fig. 5. Effect of external load on lithium zirconate particle bed effective thermal conductivity.

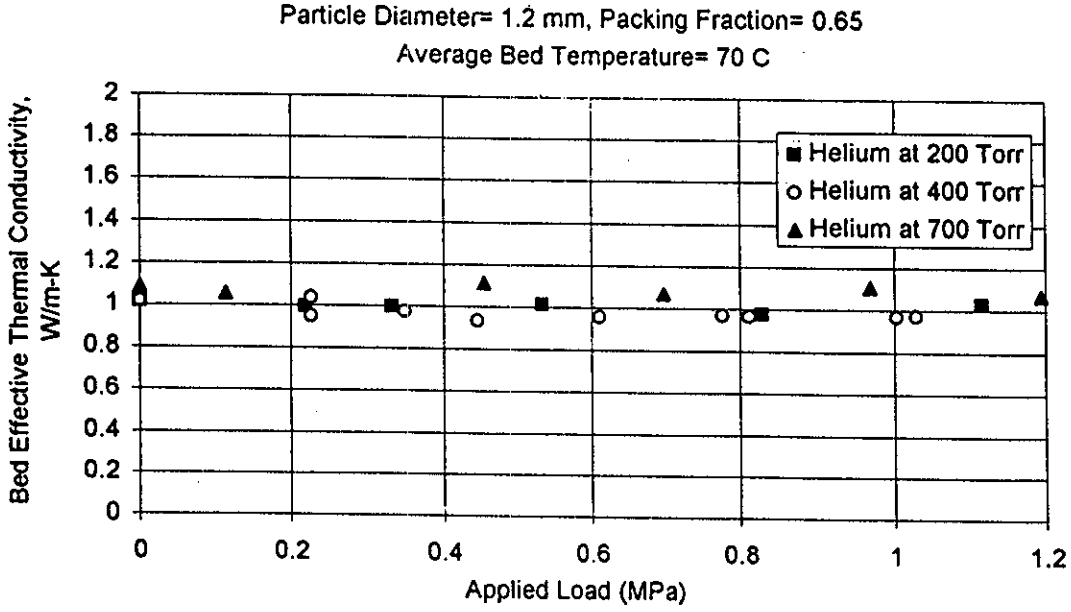

Fig. 6. Effect of external load on lithium zirconate particle bed effective thermal conductivity.

thermal conductivity at no load, is given for the three particle bed materials and as a function of the cover gas pressure. For aluminum and beryllium beds with high solid thermal conductivity (therefore, high solid-to-gas conductivity ratio), the increase in the bed effective thermal conductivity, due to the applied external load, varies from 1.72 with atmospheric helium as the cover gas to 5.8 with air at 34 Torr as the cover gas. For lithium zirconate particles, on the other hand, with a much lower solid thermal conductivity, the bed effective thermal conductivity is practically independent of the external load. The effect of external load on the effective thermal conductivity of particle beds observed in this study is in general agreement with the results of a similar study done by Duncan et al.[18]

Table III also shows the measured effective thermal conductivities of the three particle beds, with no external load, as a function of the cover gas pressure. These

TABLE III

Thermal Conductivity Ratios* of Aluminum, Lithium Zirconate, and Beryllium Particle Beds Subjected to an External Pressure of 0.68 MPa

Particle Type	Air Cover Gas Pressure (Torr)					Helium Cover Gas Pressure (Torr)			
	34	38	200	700	760	200	400	700	760
Aluminum		5.5 (0.9)[a]			3.3 (1.35)	2.04 (3.2)			1.72 (4.4)
Beryllium	5.8 (0.25)		3.1 (0.6)		2.95 (0.65)	1.96 (1.2)	1.72 (1.72)	1.93 (1.76)	
Lithium zirconate		~1.04 (0.53)			~1.1 (0.67)	~1.0 (1.0)	~1.0 (1.0)	~1.0 (1.0)	

*$(k)_{with\ load}/(k)_{no\ load}$.
[a]Measured conductivity at no load in W/m·K.

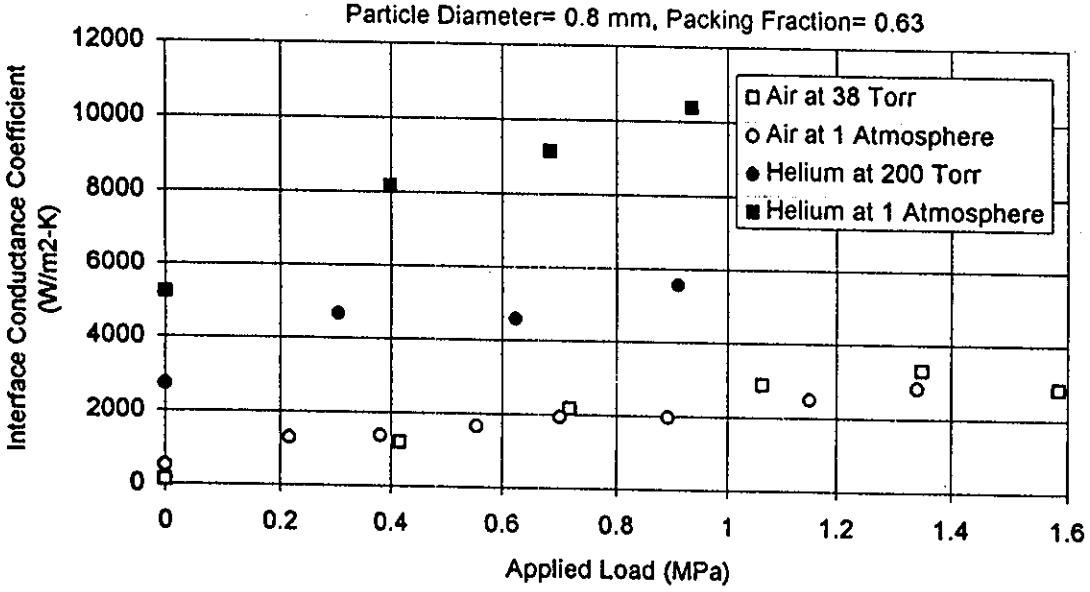

Fig. 7. Effect of external load on aluminum particle bed–stainless steel surface interface thermal conductance coefficient.

values are in reasonable agreement with those reported in Ref. 11 on aluminum and beryllium, in Ref. 12 on lithium zirconate, and in Ref. 13 on beryllium particle beds.

IV.D. Particle Bed–Stainless Steel Interface Thermal Conductance Coefficient

Figures 7 and 8 show the effect of applied external load on the bed–stainless steel interface thermal conductance coefficient. As in the case of bed thermal conductivity, the bed-wall interface thermal conductance coefficient is a strong function of the solid-to-gas conductivity ratio. For aluminum with high solid thermal conductivity, Fig. 7 shows that an increase in the applied load from 0 to 1 MPa increases the interface thermal conductance coefficient by a factor of ~2 with helium as the cover gas and by a factor of ~10 with air as the cover gas. For the lithium zirconate bed with much lower solid thermal conductivities, Fig. 8 shows that the increase in the interface thermal conductance coefficient, for applied loads in the range of 0 to 1.36 MPa with both helium and air as the cover gas, is small and within the experimental error.

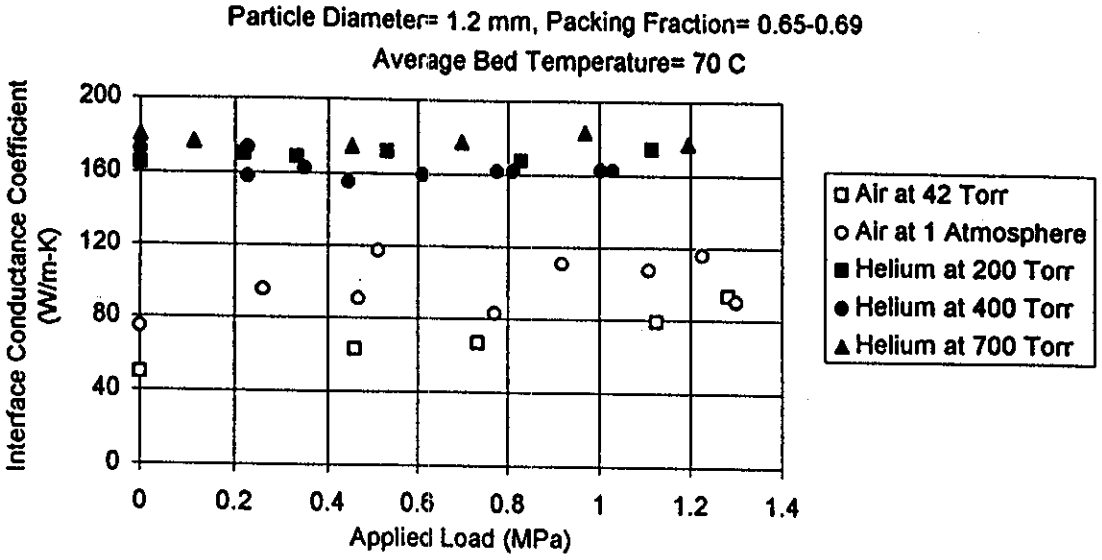

Fig. 8. Effect of external load on lithium zirconate particle bed-stainless steel surface interface thermal conductance coefficient.

IV.E. Uncertainties in the Experimental Data

Figures 9a, 10a, and 11a show the experimental effective thermal conductivities of aluminum, beryllium, and lithium zirconate particle beds with helium at 1 atm, 700 Torr, and 700 Torr, respectively, along with the experimental uncertainties in terms of error bars. For the aluminum and beryllium particle beds, the uncertainties in the effective thermal conductivity varies form 25% at 0 load to ~10% at 1.58 MPa. The uncertainty in the bed effective thermal conductivity decreases as the bed thermal conductivity increases. The uncertainties in the lithium zirconate bed effective thermal conductivities are much higher than those of aluminum and beryllium and vary from 50 to ~100%. The main contributor to the uncertainties in the measured particle beds thermal conductivities, as shown in Figs. 9b, 10b, and 11b, is the uncertainty in the calculated heat flux, which accounts for 60 to 90% of the uncertainties in the aluminum and beryllium thermal conductivities and >90% of the uncertainties in the lithium zirconate effective thermal conductivity.

IV.F. Comparison of the Experimental Results with Model Predictions

Among the several available models for predicting the particle bed effective thermal conductivity, the Bauer, Schlunder, and Zehner model[8] recommended in a recent review by Fundamenski and Gierszewski[19] was chosen for comparison with the experimental results. Figures 12a, 13a, and 14 show the experimental values as well as model predictions for beryllium particle bed effective thermal conductivities when air is used as the cover gas. Figures 15a, 16a, and 17a show the corresponding results for helium as the cover gas. The agreement between the experimental results and the model predictions, for the case of air, is excellent for applied loads <1 MPa. For the case of helium, the measured values of the bed effective thermal conductivity are 10 to 50% lower than the model predictions. Figures 12b, 13b, 15b, 16b, and 17b show the thermal conductivity ratio, defined as $(k_{eff})_{applied\ load}/(k_{eff})_{no\ load}$, as a function of the applied external load. The experimental thermal conductivity ratios are ~30 to 40% higher than the model results. In other words, the measured effect of external pressure on the bed effective thermal conductivity is higher than predicted by the model.

V. CONCLUSIONS

The effective bed thermal conductivities of aluminum, beryllium, and lithium zirconate particles with average respective diameters of 0.8, 2, and 1.2 mm, respectively, as a function of applied external load in the range of 0 to 1.5 MPa were measured. Air and helium at pressures in the range of 34 to 760 Torr were used as the cover gas. The experimental results for the beryllium particle bed were compared with those of the model predictions. The following paragraphs outline the conclusions reached.

When subjected to an external load of 1.36 MPa, with air at 1 atm and 38 Torr pressure, the aluminum bed effective thermal conductivity increased by factors of 5.2 and 7.7, respectively, relative to that with zero load. With helium at 1 atm and 200 Torr pressure, increasing the applied load from 0 to 0.95 MPa increased

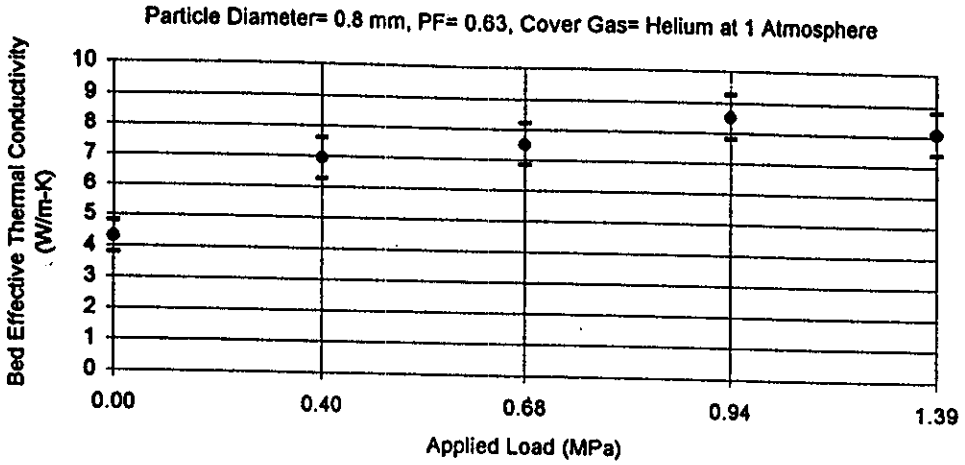

Fig. 9a. Uncertainties in the aluminum particle bed effective thermal conductivity.

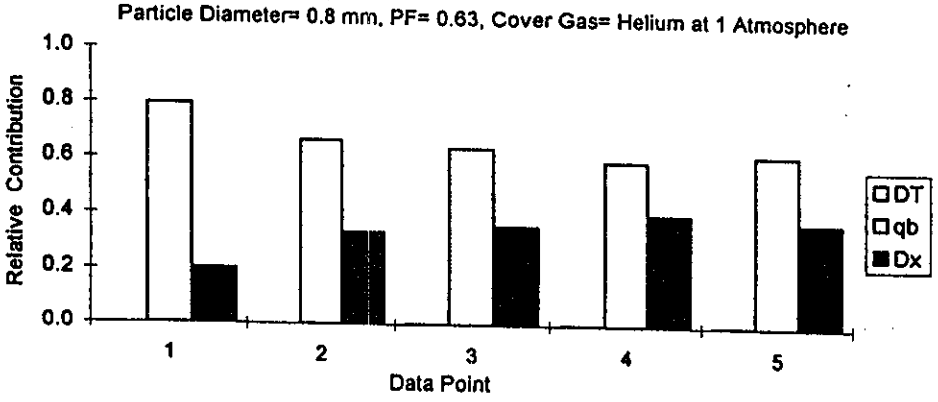

Fig. 9b. Relative contributions of uncertainties in the heat flux, temperature difference, and distance between thermocouple positions to the uncertainty in the aluminum particle bed effective thermal conductivity.

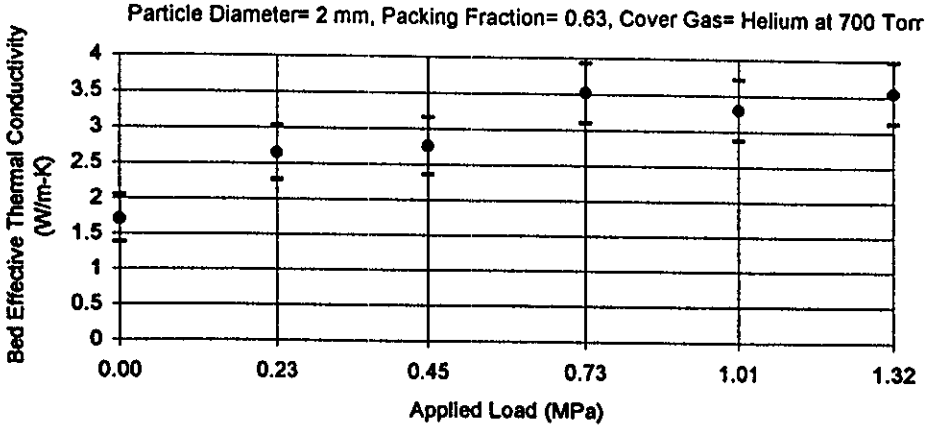

Fig. 10a. Uncertainties in the beryllium particle bed effective thermal conductivity.

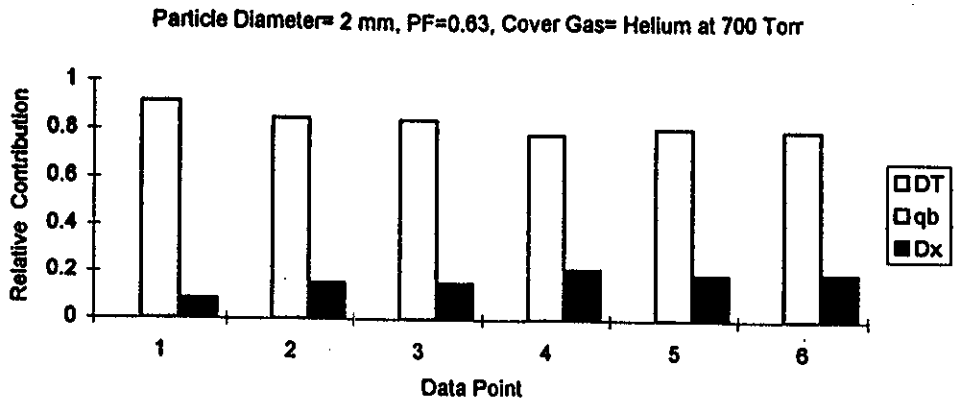

Fig. 10b. Relative contributions of uncertainties in the heat flux, temperature difference, and distance between thermocouple positions to the uncertainty in the beryllium particle bed effective thermal conductivity.

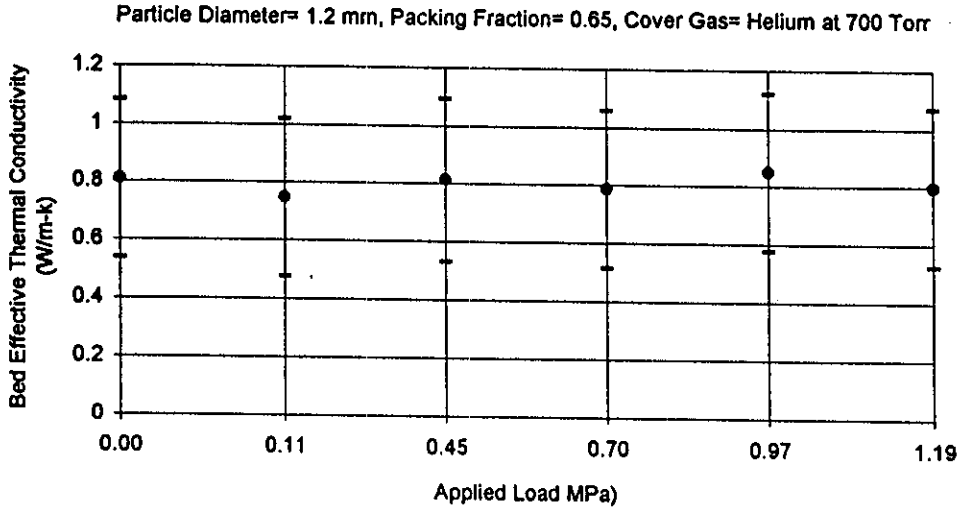

Fig. 11a. Uncertainties in the lithium zirconate particle bed effective thermal conductivity.

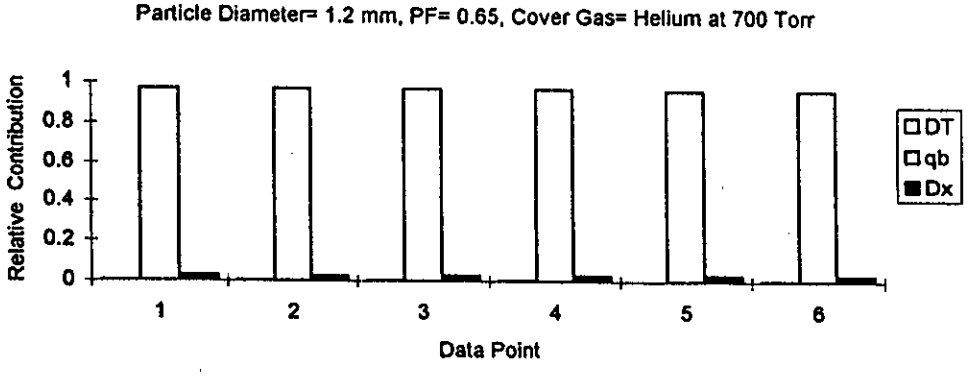

Fig. 11b. Relative contributions of uncertainties in the heat flux, temperature difference, and distance between thermocouple positions to the uncertainty in the lithium zirconate particle bed effective thermal conductivity.

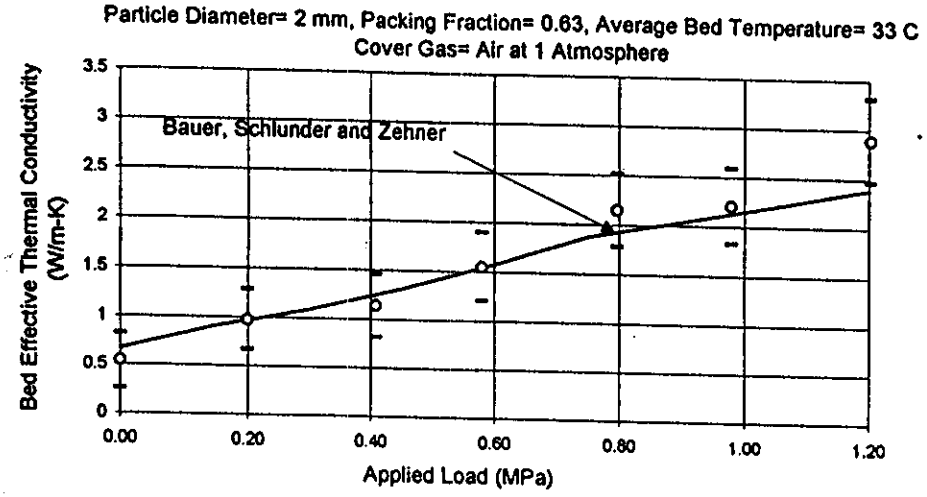

Fig. 12a. Effect of external load on beryllium particle bed effective thermal conductivity.

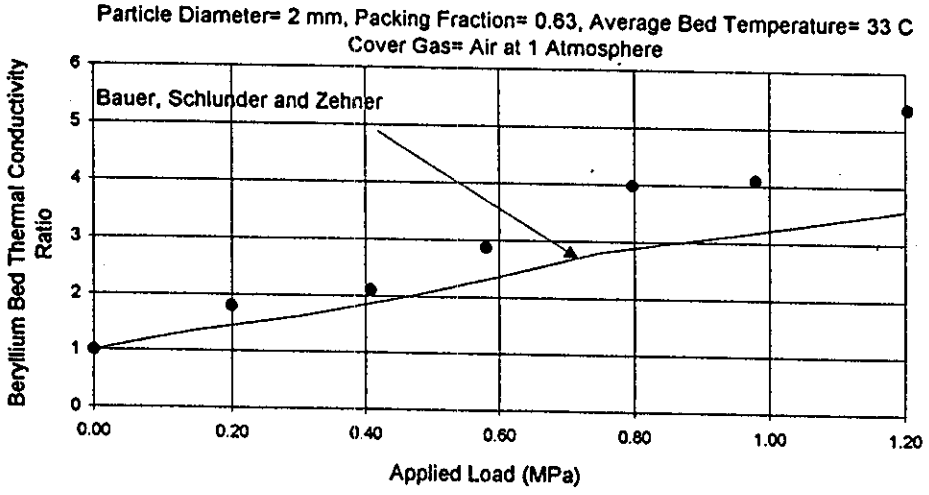

Fig. 12b. Effect of external load on beryllium particle bed effective thermal conductivity ratio.

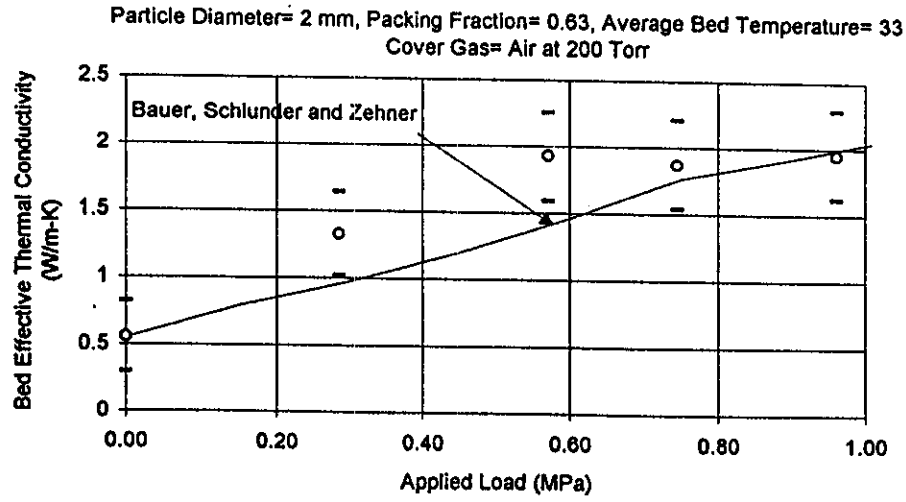

Fig. 13a. Effect of external load on beryllium particle bed effective thermal conductivity.

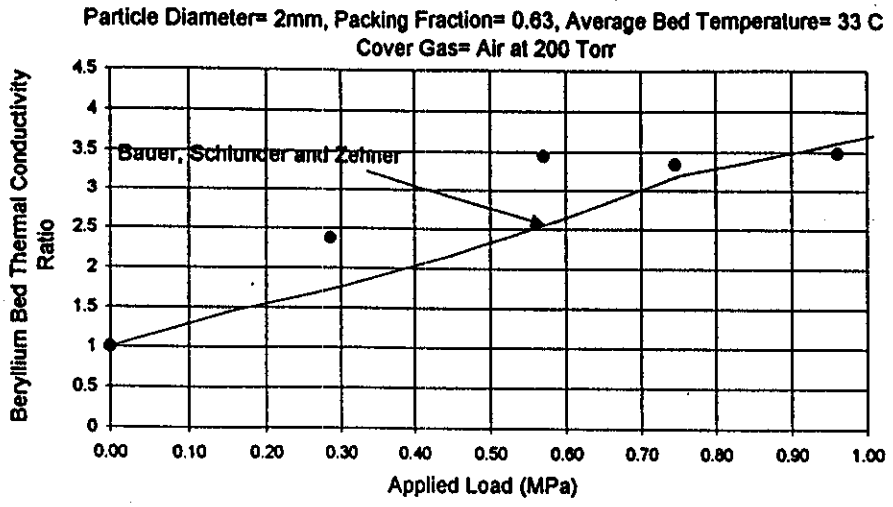

Fig. 13b. Effect of external load on beryllium particle bed effective thermal conductivity ratio.

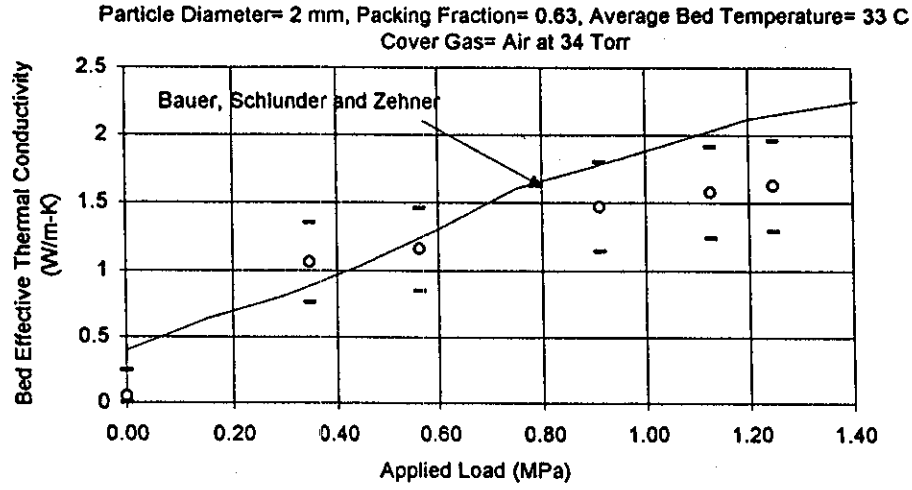

Fig. 14. Effect of external load on beryllium particle bed effective thermal conductivity.

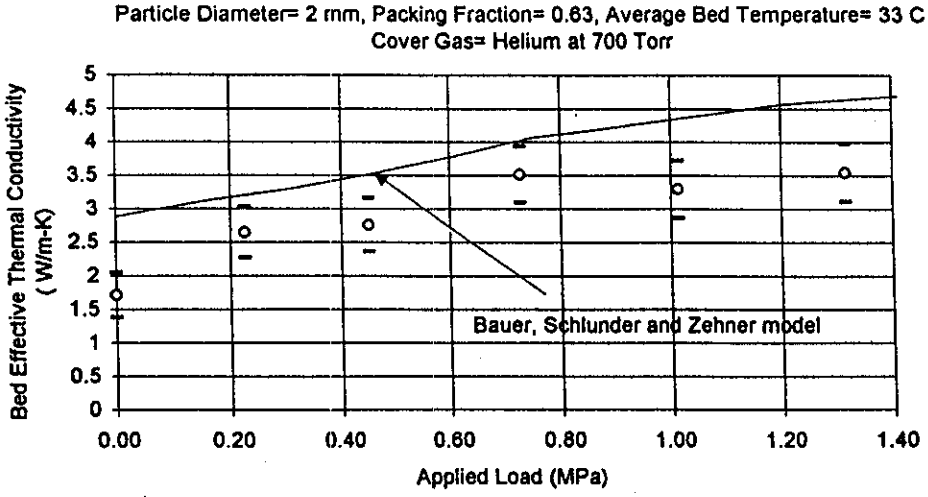

Fig. 15a. Effect of external load on beryllium particle bed effective thermal conductivity.

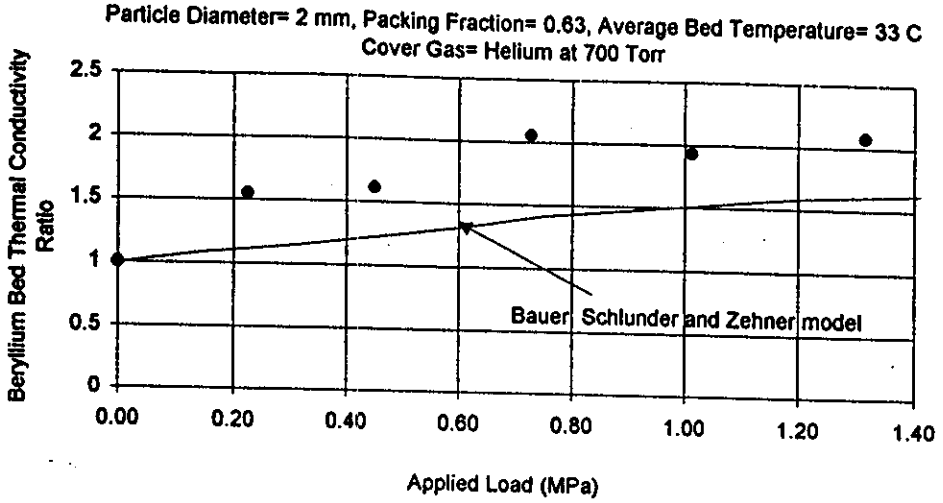

Fig. 15b. Effect of external load on beryllium particle bed effective thermal conductivity ratio.

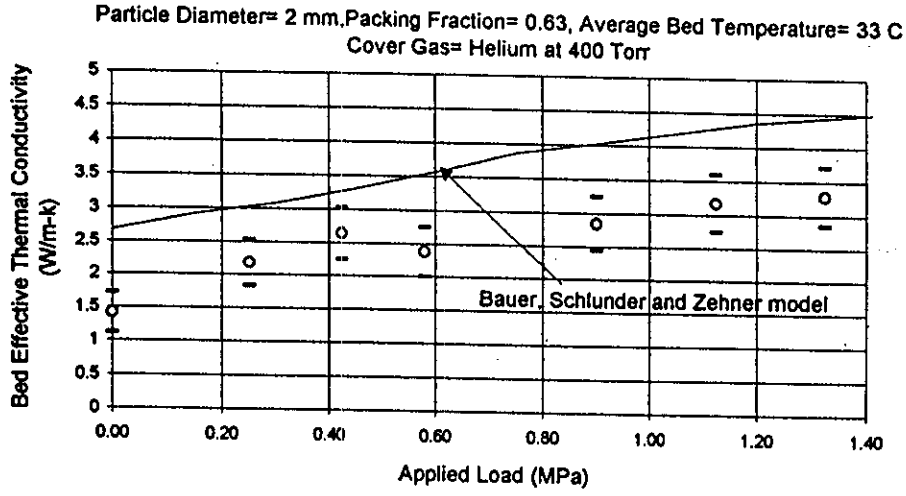

Fig. 16a. Effect of external load on beryllium particle bed effective thermal conductivity.

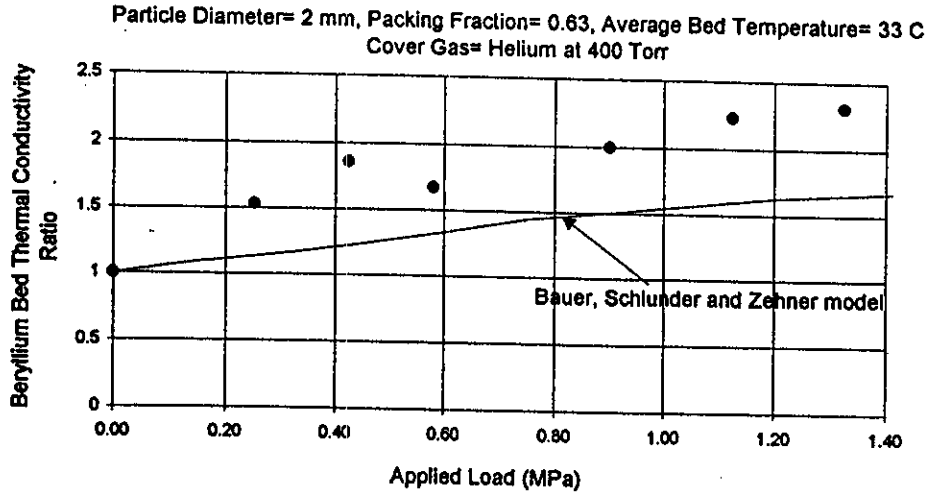

Fig. 16b. Effect of external load on beryllium particle bed effective thermal conductivity ratio.

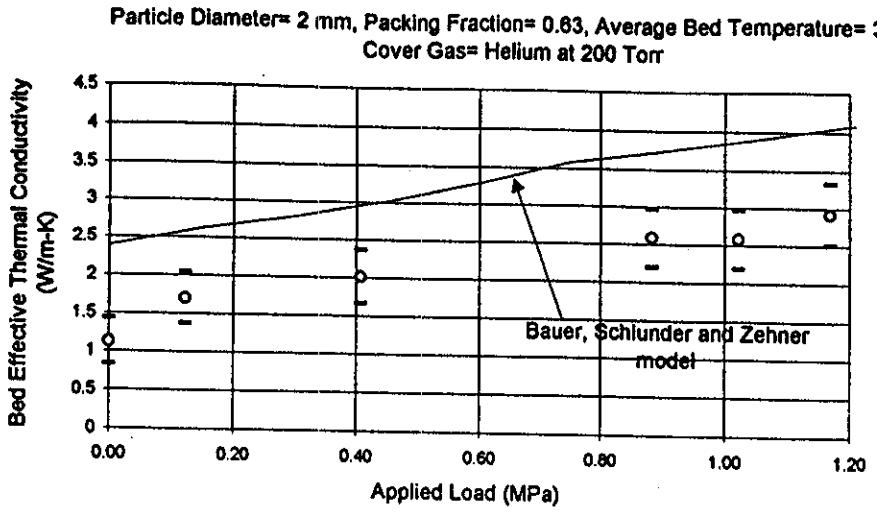

Fig. 17a. Effect of external load on beryllium particle bed effective thermal conductivity.

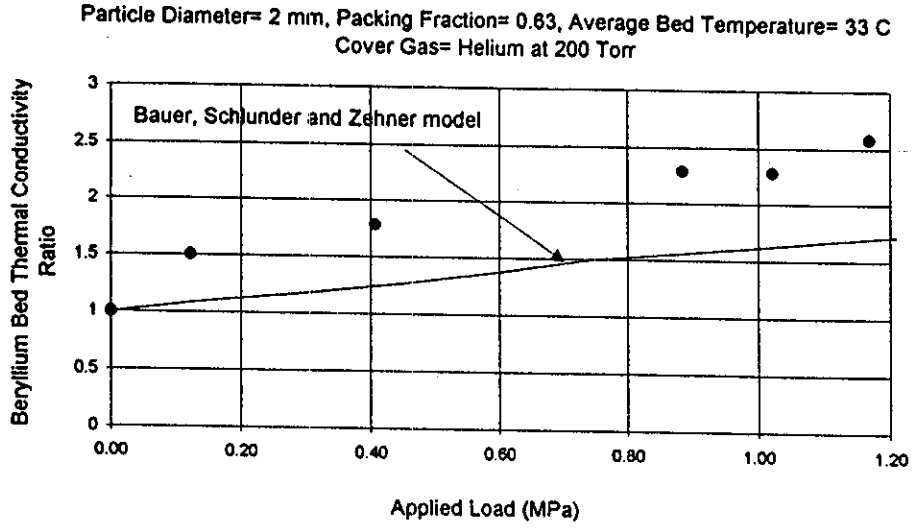

Fig. 17b. Effect of external load on beryllium particle bed effective thermal conductivity ratio.

the effective aluminum bed thermal conductivity by factors of 1.86 and 2.4, respectively.

The effective thermal conductivity of the beryllium particle bed with air at 1 atm pressure increased by a factor of 4.64 as the applied external load was raised from 0 to 1.22 MPa. For the same range of the applied load (0 to 1.22) and air at 34 Torr, the bed effective thermal conductivity increased by a factor of ~7.4. With helium at 700, 400, and 200 Torr pressures, increasing the applied load from 0 to 1.3 MPa increased the beryllium bed effective thermal conductivity by a factor of 2, 2.24, and 2.44, respectively.

The observed changes in the lithium zirconate bed [packing fraction (PF) = 69%] effective thermal conductivity when subjected to external loads of up to 1.7 MPa with air and helium as the cover gas appears to be small and within the experimental error.

Variations in the bed–stainless steel interface conductance coefficient with the applied external load closely followed those of the bed effective thermal conductivity.

In general, the effective thermal conductivity of packed beds increases when subjected to external mechanical loads. The degree of increase in the bed thermal conductivity with applied external load is a strong function of the solid-to-gas conductivity ratio.

The experimental results for the beryllium bed effective thermal conductivity compares reasonably well with those of the Bauer, Schlunder, and Zehner model with air as cover gas. However, with helium as cover

gas, the measured effect of external pressure on the bed effective thermal conductivity is higher than that predicted by the model.

REFERENCES

1. M. A. ABDOU et al., "A Helium-Cooled Solid Breeder Concept for the Tritium-Producing Blanket of the International Thermonuclear Experimental Reactor," *Fusion Technol.*, **15**, 166 (1989).

2. M. DALLE DONNE et al., "BOT Helium Cooled Solid Breeder Blanket," KfK-4929, Kernforschungszentrum Karlsruhe (Oct. 1991).

3. H. TAKATSU et al., "Layered Pebble Bed Concept for ITER Breeding Blanket," presented at 17th Symp. Fusion Technology, Rome, Italy, 1992.

4. D. L. SMITH et al., "Blanket Comparison and Selection Study," Final Report, ANL/FPP-84-1, Argonne National Laboratory (Sep. 1984).

5. M. S. TILLACK, A. R. RAFFRAY, A. Y. YING, M. A. ABDOU, and P. HUEMER, "Experimental Studies of Active Temperature Control in Solid Breeder Blankets," *Fusion Eng. Des.*, **17**, 165 (1991).

6. A. R. RAFFRAY, M. S. TILLACK, and M. A. ABDOU, "Thermal Control of Ceramic Breeder Blankets," *Fusion Technol.*, **23**, *3*, 281 (1993).

7. W. NORIAKI and K. KATO, "Effective Thermal Conductivity of Packed Beds," *J. Chem. Eng. Japan*, **2**, *1*, 24 (1969).

8. R. BAUER, E. U. SCHLUNDER, and ZEHNER, "Effective Radial Thermal Conductivity of Packings in Gas Flow. Part II. Thermal Conductivity of the Packing Fraction Without Gas Flow," *Int. Chem. Eng.*, **18**, *2*, 189 (1978).

9. R. O. A. HALL and D. G. MARTIN, "The Thermal Conductivity of Powder Beds," *J. Nucl. Mater.*, **101**, 172 (1981).

10. Z. R. GORBIS, A. R. RAFFRAY, and M. A. ABDOU, "Study of Effective Solid-to-Solid Contact Thermal Resistance and Its Application to Solid Breeder Blanket Design for ITER," *Fusion Technol.*, **19**, 1519 (1991).

11. M. DALLE DONNE and G. SORDON, "Heat Transfer in Pebble Beds for Fusion Blankets," *Fusion Technol.*, **17**, 597 (1990).

12. P. GIERSZEWSKI, Private Communication, Canadian Fusion Fuels Technology Project (1993).

13. M. ENOEDA, S. SATOH, T. TURASAWA, and H. TAKATSU, "Measurement of Effective Thermal Conductivity of Lithium Oxide and Beryllium Sphere Packed Beds" (to be published).

14. F. TEHRANIAN, "Effect of External Load on Particle Beds Thermal Properties," UCLA-FNT-68, UCLA-ENG-93-24, University of California, Los Angeles (May 1993).

15. F. TEHRANIAN, "Evaluation of the Experimental Results on the Effect of External Load on Particle Beds Thermal Properties," UCLA-FNT-72, UCLA-ENG-93-82, University of California, Los Angeles (Nov. 1993).

16. N. D. COX, "A Report on a Sensitivity Study of the Response Surface Method of Uncertainty Analysis of a PWR Model," Re-S-77-7, EG&G Idaho Inc. (Jan. 1977).

17. S. O. PEAK, "Code Development and Analysis Program," CDAP-TR-78-024, EG&G Idaho, Inc. (July 1978).

18. A. B. DUNCAN, G. P. PETERSON, and L. S. FLETCHER, "Effective Thermal Conductivity Within Packed Beds of Spherical Particles," *Trans. ASME*, **111**, (Nov. 1989).

19. W. FUNDAMENSKI and P. GIERSZEWSKI, "Heat Transfer Correlations for Packed Beds," *Fusion Technol.*, **21**, 2123 (1992).

Fatollah Tehranian (PhD, University of California, Berkeley, 1983) is a senior development engineer in the Fusion Engineering Program at the University of California, Los Angeles (UCLA) with experimental and analytical research interests in the areas of thermomechanics, heat transfer, and tritium transport as related to fusion nuclear technology.

Mohamed A. Abdou (PhD, University of Wisconsin, 1973) is a professor in the Department of Mechanical, Aerospace, and Nuclear Engineering at UCLA. He is also the leader of the Fusion Engineering Program. His research interests include fusion neutronics, thermal hydraulics, blanket technology, fusion reactor design, and system studies.